

2010

Low-Grade Waste Heat Recovery for Power Production using an Absorption-Rankine Cycle

Thomas Robbins
Georgia Institute of Technology

Srinivas Garimella
Georgia Institute of Technology

Follow this and additional works at: <http://docs.lib.purdue.edu/iracc>

Robbins, Thomas and Garimella, Srinivas, "Low-Grade Waste Heat Recovery for Power Production using an Absorption-Rankine Cycle" (2010). *International Refrigeration and Air Conditioning Conference*. Paper 1157.
<http://docs.lib.purdue.edu/iracc/1157>

This document has been made available through Purdue e-Pubs, a service of the Purdue University Libraries. Please contact epubs@purdue.edu for additional information.

Complete proceedings may be acquired in print and on CD-ROM directly from the Ray W. Herrick Laboratories at <https://engineering.purdue.edu/Herrick/Events/orderlit.html>

Low-Grade Waste Heat Recovery for Power Production using an Absorption-Rankine Cycle

Thomas Robbins¹ and Srinivas Garimella^{2*}

^{1,2}Georgia Institute of Technology, George W. Woodruff School of Mechanical Engineering,
Atlanta, GA USA
(404)-894-7479; srinivas.garimella@me.gatech.edu

* Corresponding Author

ABSTRACT

An investigation of heat recovery for power generation using an absorption-Rankine cycle with a low temperature waste heat source was conducted. In such a cycle, the condenser and boiler of a conventional Rankine system are replaced with an absorber and desorber. A recuperative solution heat exchanger is also incorporated between the absorber and desorber to minimize the external heat input. An ionic liquid-refrigerant pair is used as the working fluid, for which fluid properties were developed using the Peng-Robinson equation of state for a binary mixture. A detailed thermodynamic model of the system was developed to understand the potential of this cycle and working fluid combination. It was shown that the system is capable of achieving 15 percent conversion efficiencies using waste heat in the 130-160°C range. A parametric study also shows that the system can operate over a range of source and sink temperatures. The effects of solution heat exchanger efficiency and turbine efficiency on system performance are also investigated.

1. INTRODUCTION

This study investigated the feasibility of utilizing low grade waste heat with an Absorption-Rankine cycle for the generation of power. Many industrial applications produce large amounts of waste heat, which can be used as a source for the absorption-Rankine cycle modeled here. The proposed system uses a binary mixture of amyl acetate and carbon dioxide as the working fluid. The objective of this study is to determine whether low grade heat from industrial processes can be utilized to effectively produce power. The increasing cost of energy will make production of power from waste heat streams in industrial settings increasingly cost effective. In addition, the production of power from waste heat is environmentally neutral since it essentially does not require the use of more fuel beyond what is already used for the primary end use that produced the waste heat.

Although absorption power cycles have been considered for at least fifty years, research and applications of this technology has been rather limited. Maloney and Roberson (1953) investigated a power cycle utilizing absorption. Their design considered the use of an absorber as a condenser and a desorber as the boiler. The system used a mixture of ammonia and water as the working fluid. The performance of the system was shown to be less desirable than alternatives and further work on absorption-Rankine cycles has been limited.

Recent work has shown that room temperature ionic liquids (RTIL) show strong solvation of a number of chemicals (Anderson *et al.*, 2002). Yokozeki and Shiflett (2007) investigated the absorption of ammonia into ionic liquids. The strong ability of RTIL to form solutions makes them potentially attractive alternatives to conventional working fluid pairs considered thus far for absorption systems. These alternative absorbent pairs allow higher operating pressures at lower temperatures, with typically lower specific volumes, which could result in smaller components and higher efficiencies. The present work investigates the pairing of amyl acetate and carbon dioxide.

2. CYCLE DESCRIPTION

A schematic of the cycle with labeled state points is shown in Figure 1. State (1) represents the outlet of the solution pump. Here a concentrated solution of amyl acetate with absorbed CO_2 is pumped from the absorber to the high pressure side of the cycle. A solution heat exchanger is used to preheat the solution between state (1) and state (2). After being preheated in the solution heat exchanger, the concentrated solution flows into the desorber where it is further heated. The desorber is heated by a flow of warm fluid from either the exhaust gases or cooling system of an industrial process. The hot fluid flows into the desorber heat exchanger at point (10) and leaves the heat exchanger at point (11). In the desorber, the CO_2 is desorbed from the solution and a high pressure vapor is generated. In an actual system, depending on the operating conditions, the vapor can contain as much as 15% amyl acetate by mass. Under the conditions being considered here, this presence of amyl acetate in the vapor phase flowing through the turbine has the potential to cause condensation before the exit of the turbine, which is undesirable. The use of a

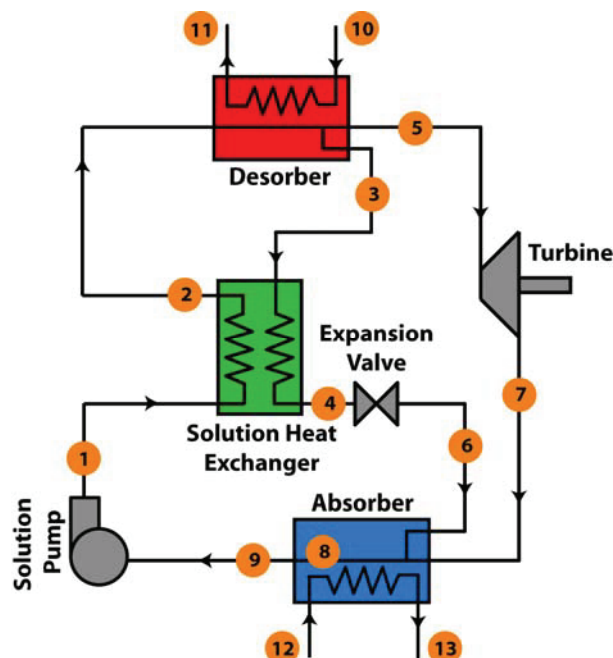


Figure 1: Absorption-Rankine Cycle

rectifier between the desorber and the turbine would supply refrigerant of a higher purity to the turbine, thus decreasing the potential for such condensation in the turbine. However, in this preliminary study, the rectifier is not included in the system. Thus, the presence of amyl acetate lowers the enthalpy of the vapor compared to the enthalpy of the vapor in a system where the amyl acetate has been removed by a rectifier. However, the larger mass flow rate of the vapor flowing through the turbine in this case without rectification compensates somewhat for the lower enthalpy, decreasing the inaccuracy of the estimation of the energy flow through the turbine due to the lack of the rectifier. The dilute solution from which the vapor has desorbed exits the desorber as a saturated liquid at state (3) and enters the solution heat exchanger. The saturated dilute solution loses heat and is substantially sub-cooled when it enters the solution expansion valve at state (4). The high pressure CO_2 vapor leaves the desorber at state (5). The vapor flows to the inlet of the turbine at state (5), where it is expanded to the low pressure state (7), providing a net work output from the system. The low pressure CO_2 vapor from (7) recombines with the dilute solution from the expansion valve outlet at state (6) in the absorber. At the lower temperature, the CO_2 is reabsorbed into the amyl acetate solution in the absorber. The absorption process is exothermic, so it is necessary to cool the solution as the CO_2 is being absorbed. This is done by using air or water at ambient conditions entering the absorber heat exchanger at state (12) and exiting at state (13). The concentrated solution is at a saturated state in the absorber at (8). Finally, the solution is sub-cooled to state point (9) at the absorber outlet and flows to the pump inlet. The concentrated solution enters the pump at state (9) to complete the cycle.

3. EQUATION OF STATE MODELING

To model this system, the Peng-Robinson (PR) equation of state was implemented to determine the properties of the fluid mixture at each state point. Modeling was done using the non-linear equation solving capabilities of *Engineering Equation Solver* (EES) (Klein, 2009) and its included Peng-Robinson library. The PR uses the critical pressure and temperature of each fluid and an experimentally determined acentric factor, ω , to determine the properties of the fluid (Peng and Robinson, 1976). Additionally, an experimentally determined interaction term is used between each fluid in a mixture. If P represents the pressure, T is the temperature of the fluid, v is the specific volume, b is a constant determined by the critical pressure and temperature, and a function of the system temperature and the acentric factor, the PR equation of state is as follows (Peng and Robinson, 1976):

$$P = \frac{RT}{v-b} - \frac{\alpha(T, \omega)}{v(v+b) + b(v-b)} \quad (1)$$

This equation is more commonly expressed in terms of the compressibility factor of the fluid as:

$$Z^3 - (1-B)Z^2 + (A-3B^2-2B)Z - (AB-B^2-B^3) = 0 \quad (2)$$

where

$$A = \frac{aP}{(R^2T^2)} \quad (3)$$

$$B = \frac{bP}{RT} \quad (4)$$

$$Z = \frac{Pv}{RT} \quad (5)$$

There are alternatively three real roots or one real root to the above equations. The one solution case represents the situation when the fluid is only in one phase, while the case of three solutions represents the case where two phases exist at the given conditions. The largest compressibility represents the gaseous phase while the smallest compressibility represents the liquid phase. The middle value has no real physical meaning (Kyle, 1992).

For a mixture such as the amyl acetate-carbon dioxide mixture being modeled here, the properties are determined based upon the summation of the properties of the components weighted by the molar fraction of each component in the mixture and an experimentally determined interaction term, k_{ij} , between fluids according to the equations (Kyle, 1992) for an arbitrary number of fluids C:

$$b = \sum_{i=1}^C \chi_i b_i \quad (6)$$

$$a = \sum_{i=1}^c \sum_{j=1}^c \chi_i \chi_j a_{ij} \quad (7)$$

3.1 Phase Compositions

Using these composite values, the PR equation can be used to determine the properties of the mixture, if the mass fraction of each component of the mixture is known. However, if two phases exist at a given condition, it is necessary to determine the fugacity and set it equal for the gas and liquid phase of each component in the system to determine the composition of each phase (Kyle, 1992).

3.2 Enthalpy and Entropy Calculations

The enthalpy and entropy of a mixture are calculated with the Peng-Robinson equation using offset functions (Reid *et al.*, 1987). The offset function predicts how the enthalpy and entropy of the mixture will differ from an ideal gas at a fixed pressure, or fixed specific volume, and the same temperature as the mixture. If the specific heat under constant pressure is known for each of the components, the value of the ideal gas enthalpy and entropy can be used with the offset function to determine the enthalpy and entropy of the mixture. The enthalpy and entropy offset equations are shown in equations (8) and (9), respectively:

$$h = h_{id} - RT(1-Z) + \frac{T}{2\sqrt{2}b} \frac{da}{dT} - a \ln\left(\frac{Z+2.41B}{Z-0.41B}\right) \quad (8)$$

$$s = s_{id} + R \ln(Z-B) + \frac{1}{2\sqrt{2}b} \frac{da}{dT} \ln\left(\frac{Z+2.41B}{Z-0.41B}\right) \quad (9)$$

The differential of a with respect to temperature was determined using the DSADT_MIX_PR function within the Peng-Robinson external library in EES. Here h_{id} is the enthalpy of an ideal gas under the same conditions, while s_{id} is the entropy of an ideal gas under the same conditions.

4. BASELINE SYSTEM MODEL

The thermodynamic state point model developed in EES was run with a set of assumed inputs corresponding to expected system operating conditions. A desorber solution outlet temperature of 150°C was assumed, while the absorber concentrated solution saturation temperature was chosen to be 25°C, with 5°C of sub-cooling from the absorber to the pump inlet. It should be noted that small changes in the temperature of the system can greatly affect the mass fraction of CO₂ absorbed into the amyl acetate. The impact of changing system conditions is quantified and discussed in the next section.

An isentropic efficiency of 85% for the turbine and 90% for the solution pump were assumed. The effectiveness of the solution heat exchanger was assumed to be 85%. The expansion of the liquid between state (4) and state (6) was assumed to be isenthalpic.

The high side pressure was assumed to be 15.9 MPa, while the low side pressure was assumed to be 5.4 MPa. These pressures correspond to pressures that enable the required absorption and desorption at the chosen absorber and desorber temperatures. The mass flow rate through the pump was fixed at 0.18 kg/s, which corresponds to a net power output of 5.04 kW at these system pressures. The required pumping power for the system at these conditions is 2.32 kW. (The power required from the pump is the product of the pressure difference and the volumetric flow rate of the fluid.) Table 1 summarizes these baseline conditions.

Table 1. Baseline Conditions

Name	Baseline	Name	Baseline
High Side Pressure	15.9 MPa	Solution Pump Flow Rate	0.18 kg/s
Low Side Pressure	5.4 MPa	Turbine Efficiency	85%
Absorber Solution Saturated Outlet	25°C	Solution Pump Efficiency	90%
Desorber Solution Outlet	150°C	Solution Heat Exchanger Effectiveness	85%
Pump Power	2.32 kW	Net Power Output	5.04 kW

4.1 Desorber

Waste heat either in the form of hot gases or hot water from another process transfers heat to the amyl acetate-carbon dioxide solution in the desorber. At the baseline conditions, the concentrated solution enters the desorber from the solution heat exchanger at a 65.7% mass fraction of CO₂ at a temperature of 72.7°C. A heat input of 36 kW from the waste heat stream increases the temperature of the solution to 150°C as desorption proceeds, producing a CO₂-absorbent vapor mixture. The vapor leaves the desorber and enters the turbine with a flow rate of 0.106 kg/s and at a concentration of 82.3% CO₂. The saturated dilute solution from the desorber flows to the solution heat exchanger at a flow rate of 0.074 kg/s and a CO₂ concentration of 41.9%.

4.2 Turbine

High pressure vapor from the desorber expands through the turbine to the low pressure side. The vapor expansion produces 7.36 kW of power output while undergoing a 10.5 MPa drop in pressure. The incoming gas enters at a concentration of 82.3% CO₂ at 150°C and 15.9 MPa. It leaves the turbine at a pressure of 5.4 MPa and a temperature of 79.7°C. An enthalpy drop of 69.8 kJ/kg occurs between the inlet and the outlet of the turbine. For the cycle configuration considered here, amyl acetate would begin to condense as the gas expands through the turbine. To prevent degradation of the turbine blades without substantial modifications to source and sink conditions, a rectifier will be necessary upstream of the turbine to purify the CO₂ stream in an actual implementation of this system.

4.3 Expansion Valve

To reduce the pressure of the dilute solution from the high side pressure of 15.9 MPa to the low side pressure of 5.4 MPa, an expansion valve is used downstream of the solution heat exchanger. In this model, the valve is assumed to be isenthalpic. No flashing of the solution occurs through the expansion valve due to the cooling of the liquid in the solution heat exchanger upstream of the valve. The mass flow rate through the valve is 0.074 kg/s with a concentration of 41.9% carbon dioxide.

4.4 Absorber

Dilute solution from the expansion valve and the two-phase mixture (with a vapor quality of 80%) from the turbine outlet combine in the absorber. The dilute solution absorbs the vapor from the turbine and releases heat. In the absorber, the solution is cooled to a temperature of 25°C by heat rejection to the environment, with absorption resulting in a solution concentration of 65.7% CO₂. An additional sub-cooling of 5°C beyond the saturation condition is assumed in the absorber before the concentrated solution of CO₂ flows to the pump. The absorber requires 30.9 kW of cooling.

4.5 Solution Pump

The solution pump raises the concentrated solution from the low-side pressure to the high-side pressure of the cycle. The pump is assumed to operate at 90% of an ideal isentropic efficiency. The solution pump provides a mass flow rate of 0.18 kg/s at a power of 2.32 kW for the baseline case. The solution enters from the absorber at a temperature of 20°C and leaves the pump to enter the solution heat exchanger at 26°C.

4.6 Overall System Performance

The system efficiency for this model is defined as the net power output divided by the total heat input at the desorber:

$$\eta_{\text{system}} = \frac{\dot{W}_{\text{turb}} - \dot{W}_{\text{pump}}}{\dot{Q}_{\text{desorb}}} \quad (9)$$

The net power output is the difference between the work produced in the turbine, \dot{W}_{turb} , and the work required to pump the fluid from the low side to the high side, \dot{W}_{pump} . The heat input at the desorber is, \dot{Q}_{desorb} . For the baseline conditions, the system produces a net power output of 5.04 kW and requires 35.6 kW of heat at the desorber. The system also requires 30.9 kW of cooling at the absorber. The system efficiency for the baseline case is therefore 14.2%.

5. PARAMETRIC INVESTIGATION RESULTS

A parametric study was conducted to understand the effect of turbine efficiency, desorber temperature, absorber temperature, and solution heat exchanger effectiveness on the system performance. For each of the parameters, the net work output and the efficiency of the system were computed.

5.1 Turbine Efficiency

The turbine efficiency was varied from 50% to 95%, while the rest of the system was kept at the baseline conditions shown in Table 1. As can be expected, the work output and the efficiency of the system showed a positive linear dependence on turbine efficiency. These results are shown in Figure 2.

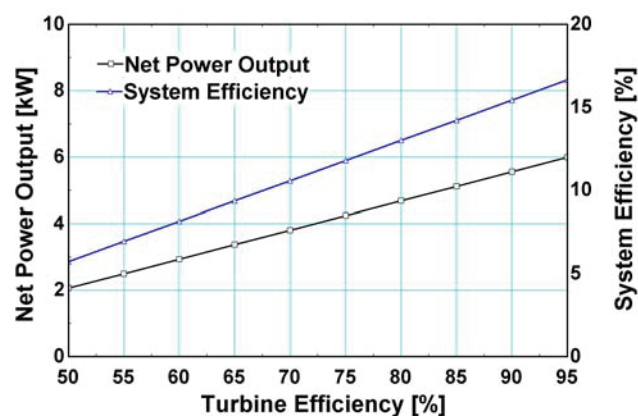


Figure 2: Net work output and system efficiency as a function of turbine efficiency

At a turbine efficiency of 50%, the net system output is only 2.06 kW, compared to the net power output of 5.98 kW with a 95% efficient turbine. The system efficiency varies from a maximum of 16.6% at a turbine efficiency of 95% to a minimum of 5.7% at the lowest turbine efficiency of 50%.

5.2 Desorber Temperature

The desorber temperature was varied from 150°C to 102.3°C, below which desorption will not take place at the specified high-side pressure. The results of varying the desorber temperature can be seen in Figure 3. The system efficiency is strongly dependent upon the desorber temperature and it can be seen that the system will operate down to 103°C, but below approximately 108°C the efficiency of the system becomes negative, as more pumping power is required to move the fluid than is being produced by the small amount of desorbed vapor. The system efficiency varies from a maximum of 14.2% at a desorber temperature of 150°C to -40.1% at 103°C. The net power output over the same range varies from 5 kW to -2.2 kW. A negative net power is due to the solution pump requiring more energy than the turbine produces.

5.3 Absorber Temperature

The absorber saturated solution outlet temperature was varied from 20°C to 50°C. With increasing absorber temperature, the efficiency and the work from the system steadily decrease. This is primarily because varying the absorber temperature also causes the low-side pressure to vary, due to the increased pressure required to cause absorption. Figure 4 shows the results of the changing the absorber temperature.

For the parametric study of absorber temperature, pump work was not fixed as in the prior analyses. Rather, the high-side pressure was specified. This was done because with a fixed pumping power, the increasing low side pressure caused by higher temperatures in the absorber resulted in high side pressures at which desorption would not occur. The pump work varied from 2.4 kW at the 20°C to 1.6 kW at 50°C. Figure 5 shows the variation in low side pressure in the absorber used for the analysis.

The net power output is at a maximum of 5.6 kW at the lowest absorber temperature, 20°C, and falls to 2.45 kW at an absorber temperature of 50°C. The system efficiency varies from 15.4% at 20°C to 8.7% at 50°C.

5.4 Solution Heat Exchanger Effectiveness

The solution heat exchanger effectiveness was varied from 50% to 95%. The solution heat exchanger does not affect the net power output from the system because the heat input at the desorber increases as the solution heat exchanger effectiveness

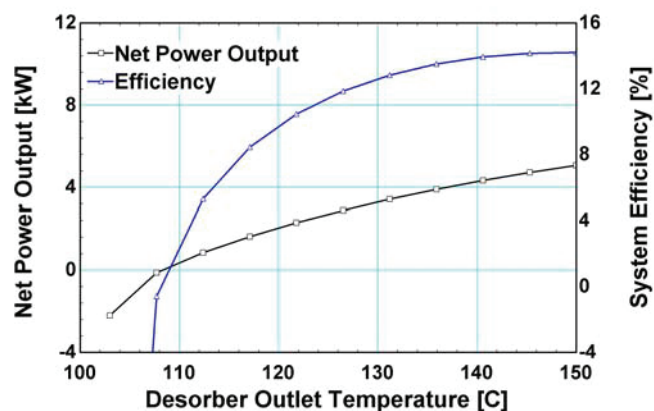


Figure 3: Net power output and system efficiency as a function of desorber temperature

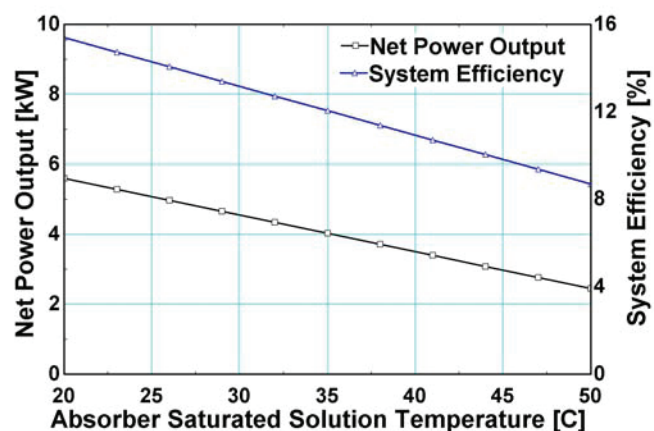


Figure 4: Net power output and system efficiency as a function of absorber temperature

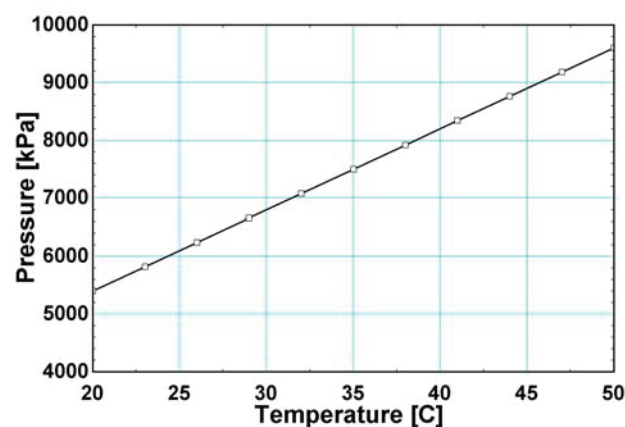


Figure 5: Absorber pressure dependence on absorber temperature.

decreases to compensate for the lower temperature incoming fluid. Additionally, the heat removed at the absorber is likewise increased with decreasing heat exchanger efficiency. The maximum system efficiency of 15.1% is achieved when the solution heat exchanger operates at 95% efficiency. When the solution heat exchanger operates at 50% efficiency, the system efficiency drops to 11.7%.

Results for the system efficiency are shown in Figure 6. The heat transferred from the heat exchanger varies from 15.4 kW in the 95% efficient case down to 8.1 kW in the 50% efficient case. It can be seen that system performance is not as heavily dependent upon the heat exchanger as it is upon the other factors, although improved heat exchanger design does play an important part in increasing the efficiency of the cycle.

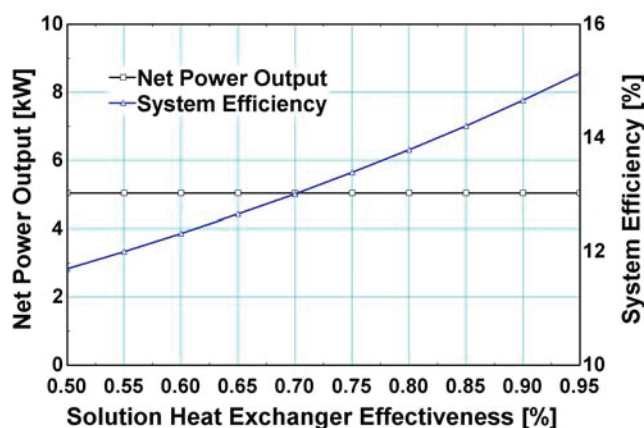


Figure 6: Net power output and system efficiency as a function of solution heat exchanger effectiveness

6. CONCLUSIONS

The use of an absorption-Rankine cycle for production of power from waste heat was modeled. Fluid properties for the working fluid pair (amyl acetate and carbon dioxide) were estimated using the Peng-Robinson equation of state. The performance of the system was evaluated for a baseline case with a nominal net power of 5 kW at a desorber temperature of 150°C and an absorber at 25°C. The system was found to operate with an efficiency of 14.2% at the baseline conditions. It requires 2.3 kW of pumping power and a heat input of 36 kW. The system requires 30.9 kW of cooling at the absorber. If the heat driving this system would otherwise be wasted, this is a feasible system for producing power to either run motors directly within a plant or to produce electricity.

Parametric studies on turbine efficiency, desorber temperature, absorber temperature, and heat exchanger effectiveness showed that it is possible to operate this system over a range of conditions. As might be expected, the efficiency of the turbine and the effectiveness of the solution heat exchanger should be maximized for the best performance. The absorber and desorber results are less intuitive and more revealing, as they help define the range over which the system can operate effectively. Although the power output decreases with decreasing desorber temperature, the system efficiency stays nearly constant as the desorber outlet temperature decreases to 135°C; losing less than 1% of the system efficiency. Furthermore, the system is still more than 8% efficient at temperatures as low as 120°C. Therefore, the absorption-Rankine system can still perform at temperatures below the baseline. Operation at low desorber temperatures allows a range of waste heat sources to be utilized, including perhaps solar thermal sources. With additional adjustments to the system, such as incorporation of a rectifier, it should be possible to increase the operation range and to optimize the system performance for a given source temperature. Likewise, the system will operate with higher absorber temperatures than those given in the base case. The range of suitable absorber temperatures is similar to the range of desorber temperatures. Only if the absorber temperature is above 55°C, 30 degrees above the base case temperature, does the system efficiency decrease below 8%. Thus, the proposed absorption-Rankine cycle for energy recovery from waste heat is viable and merits further investigation and optimization beyond what has been completed here.

NOMENCLATURE

			Subscripts	
a	PR Equation Coefficient	(Pa·m ⁶ /kg ²)	i,j	Fluid index
A	PR Equation Coefficient	(-)	id	Ideal gas
b	PR Equation Coefficient	(m ³ /kg)		
B	PR Equation Coefficient	(-)		
h	Enthalpy	(kJ/kg)		
k	Interaction Coefficient	(-)		

N	Number	(-)
P	Pressure	(Pa)
\dot{Q}_{desorb}	Heat input	(kW)
R	Gas Constant	(m ³ -Pa/K-kg)
s	Entropy	(kJ/kg-K)
T	Temperature	(°C)
\dot{W}_{pump}	Pump Work	(kW)
\dot{W}_{turb}	Turbine Work	(kW)
Z	Compressibility Ratio	(-)
v	Specific Volume	(m ³ /kg)
η	System Efficiency	(-)
χ	Molar Fraction	(mol/mol)

REFERENCES

- Anderson, J. L., J. Ding, T. Welton and D. W. Armstrong (2002), "Characterizing Ionic Liquids on the Basis of Multiple Solvation Interactions," *Journal of the American Chemical Society* Vol. 124(47) pp. 14247-14254.
- Klein, S. A. (2009). *Engineering Equation Solver, F-Chart Software*. Madison, WI.
- Kyle, B. G. (1992). *Chemical and Process Thermodynamics*. 2nd Ed. Englewood Cliffs, Simon & Schuster Company.
- Maloney, J. D. and R. C. Robertson (1953). Thermodynamic Study of Ammonia - Water Heat Power Cycles. *Oak Ridge National Laboratory*. Oak Ridge, Tennessee.
- Peng, D.-Y. and D. B. Robinson (1976), "A New Two Constant Equation of State," *Industrial Engineering Chemistry* Vol. 15(1) pp. 59-64.
- Reid, R. C., John M. Prausnitz and B. E. Poling (1987). *The Properties of Gases and Liquids*. 4th Ed. New York, McGraw-Hill.
- Yokozeki, A. and M. B. Shiflett (2007), "Vapor-Liquid Equilibria of Ammonia + ionic Liquid Mixtures," *Applied Energy* Vol. 84(12) pp. 1258-1273.